Impact of Lateral Alignment on the Energy Savings of a Truck Platoon

Preprint

Michael P. Lammert,[1] Brian McAuliffe,[2] Patrick Smith,[3] Arash Raeesi,[2] Mark Hoffman,[3] and David Bevly[3]

1 National Renewable Energy Laboratory
2 National Research Council Canada
3 Auburn University

Prepared for the WCX 2020 World Congress Experience
April 21-23, 2020

NREL is a national laboratory of the U.S. Department of Energy
Office of Energy Efficiency & Renewable Energy
Operated by the Alliance for Sustainable Energy, LLC

This report is available at no cost from the National Renewable Energy Laboratory (NREL) at www.nrel.gov/publications.

Contract No. DE-AC36-08GO28308

Conference Paper
NREL/CP-5400-78216
November 2020

Impact of Lateral Alignment on the Energy Savings of a Truck Platoon

Preprint

Michael P. Lammert,[1] Brian McAuliffe,[2] Patrick Smith,[3] Arash Raeesi,[2] Mark Hoffman,[3] and David Bevly[3]

1 National Renewable Energy Laboratory
2 National Research Council Canada
3 Auburn University

Suggested Citation
Lammert, Michael P., Brian McAuliffe, Patrick Smith, Arash Raeesi, Mark Hoffman, and David Bevly. 2020. *Impact of Lateral Alignment on the Energy Savings of a Truck Platoon: Preprint*. Golden, CO: National Renewable Energy Laboratory. NREL/CP-5400-78216. https://www.nrel.gov/docs/fy21osti/78216.pdf.

NREL is a national laboratory of the U.S. Department of Energy
Office of Energy Efficiency & Renewable Energy
Operated by the Alliance for Sustainable Energy, LLC

This report is available at no cost from the National Renewable Energy Laboratory (NREL) at www.nrel.gov/publications.

Contract No. DE-AC36-08GO28308

Conference Paper
NREL/CP-5400-78216
November 2020

National Renewable Energy Laboratory
15013 Denver West Parkway
Golden, CO 80401
303-275-3000 • www.nrel.gov

NOTICE

This work was authored in part by the National Renewable Energy Laboratory, operated by Alliance for Sustainable Energy, LLC, for the U.S. Department of Energy (DOE) under Contract No. DE-AC36-08GO28308. Funding provided by the U.S. Department of Transportation (DOT) - Federal Highway Administration under Agreement IAG-19-02109. The views expressed herein do not necessarily represent the views of the DOE or the U.S. Government. The U.S. Government retains and the publisher, by accepting the article for publication, acknowledges that the U.S. Government retains a nonexclusive, paid-up, irrevocable, worldwide license to publish or reproduce the published form of this work, or allow others to do so, for U.S. Government purposes.

Cover Photos by Dennis Schroeder: (clockwise, left to right) NREL 51934, NREL 45897, NREL 42160, NREL 45891, NREL 48097, NREL 46526.

Impact of Lateral Alignment on the Energy Savings of a Truck Platoon

Abstract

A truck platooning system was tested using two heavy-duty tractor-trailer trucks on a closed test track to investigate the sensitivity of intentional lateral offsets over a range of intervehicle spacings. The fuel consumption for both trucks in the platoon was measured using the SAE J1321 gravimetric procedure while travelling at 65 mph and loaded to a gross weight of 65,000 lb. In addition, the SAE J1939 instantaneous fuel rate was calibrated against the gravimetric measurements and used as proxy for additional analyses. The testing campaign demonstrated the effects of intervehicle gaps, following-vehicle longitudinal control, and manual lateral control. The new results are compared to previous truck-platooning studies to reinforce the value of the new information and demonstrate similarity to past trends. Fuel savings for the following vehicle was observed to exceed 10% at closer following distances. The results showed that energy savings generally increased in a non-linear fashion as the gap was reduced. The impact of different following-truck lateral offsets had a measurable impact, with up to 4% reduction in total fuel-savings (relative to an isolated vehicle condition) observed for offsets up to 1.3 m. The fuel-consumption savings on the straight segments of the track exceeded those on the curved segments by upwards of 6% and highlight some potential differences expected between close-track testing and on-highway use.

Keywords: adaptive cruise control (ACC), cooperative ACC (CACC), heavy-duty truck platooning, heavy-duty truck partial automation, vehicle control performance, heavy-duty truck fuel economy, connected and automated vehicle, vehicle alignment

Introduction

A benefit of truck platooning is the energy savings that are possible with electronically connected trucks travelling safely in close proximity to effectively share the aerodynamic load. This has been previously highlighted by numerous studies investigating truck platooning. Wind-tunnel studies [1, 2, 3, 4] and track-based fuel-economy studies [5, 6, 7, 8, 9, 10, 11, 12, 13, 14, 15] have identified trends in aerodynamic drag reduction associated with vehicles in close proximity and linked them to the resulting fuel savings. Based on previous investigations, the fuel savings associated with truck platooning and close-proximity driving has been attributed to an aerodynamic influence, but the sensitivity to vehicle alignment has not been investigated in a track study. There is some question whether unintentional driver misalignment could reduce expected fuel savings and thus require a SAE level 2 or 3 system to control the vehicle alignment well enough to achieve platooning savings over the entirety of a driver's in-service hours. Some computational studies [12] and wind-tunnel studies [3, 4] have looked at misalignment. While the computational study [12] denoted a large potential decrease in performance with as little as a 0.6 m (2 ft) offset, the wind-tunnel studies showed measurable but smaller reductions in the aerodynamic platooning benefit, particularly for offset that represents the possible motion within a lane width. The current work addresses this question at full scale on a test track to expand the knowledge of factors that can influence platoon energy savings on the road.

This paper is the first in a series that focuses on a track-based investigation of the fuel savings of a truck platoon with increasing levels of real-world complexity. The intention is to identify the variability of energy savings for truck platoons that must be accounted for when modelling the large-scale environmental benefits of introducing these systems into North American highway networks. These track tests provide controlled conditions to reliably estimate and model the potential for energy savings while systematically introducing the complexities encountered on general roadways. The second paper in this series [16] examines the influence of mixed traffic on the fuel-savings benefits of a two-truck platoon.

Background and Methods

CACC System Description

The cooperative adaptive cruise control (CACC) system allows for automated longitudinal control of a platooning vehicle. This system has been previously documented in [17] and [18], but an overview is provided here. Overall, there are several hardware and software components that make up the system. The system components are shown in Figure 1 and summarized below.

A rugged, industrial computer running the Linux operating system is the central component. The computer is the main processing unit and receives all the sensor data from the Dedicated Short Range Communications (DSRC), global positioning system (GPS), RADAR, and a J1939 controller area network (CAN) bus. The system software is also compiled and executed on this computer. The software components include the sensor drivers, CACC platooning algorithms, and the vehicle interface for automated control. These components are implemented using the Robot Operating System (ROS) middleware [19]. DSRC radios are used for vehicle-to-vehicle (V2V) communication. GPS and vehicle state information, such as vehicle speed, acceleration, and brake status are communicated amongst platooning vehicles. Although each vehicle receives all V2V data, only data from a preceding vehicle are used for estimation/control. A dual-frequency GPS receiver is used for position information. Raw GPS observables, the pseudorange and carrier phase, are also used for differential GPS relative positioning as described in [18]. The output of the GPS algorithm is a relative position vector that can be resolved into a range measurement. A forward-facing RADAR is used to provide higher frequency range, range rate, and bearing (angular offset) measurements. The RADAR measurements are combined with the relative positioning GPS solution to produce the range estimates used for longitudinal control. The RADAR is also used to track neighboring vehicles for cut-in detection between platooning vehicles.

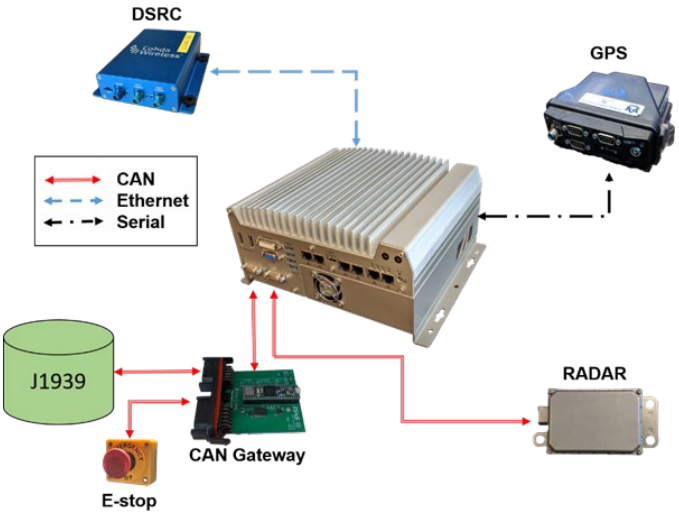

Figure 1: CACC system hardware components.

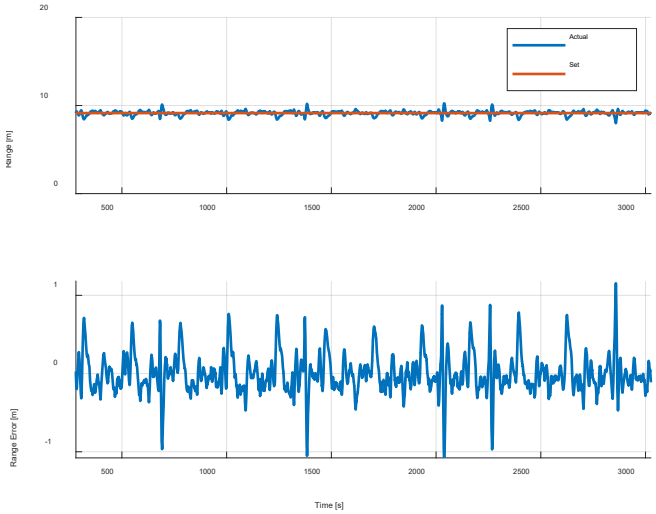

Figure 2: Longitudinal controller performance while platooning.

The longitudinal controller described in [18] calculates the desired actuation needed to track the reference following distance. In particular, the actuation commands are the desired engine torque, retarder torque, and brake rate. Automated vehicle control is achieved by taking these control commands, generating the respective CAN messages, and sending them over the vehicle's CAN bus to the appropriate electronic control unit. This process uses a vehicle specific software interface to communicate to the vehicle's stock electronic control units. Vehicle state information, such as the fuel rate, is also read through this interface as well.

A device called the CAN Gateway is connected between the computer's CAN bus and the rest of the vehicle. The CAN Gateway is used as a physical disconnect for the CACC system from the vehicle. An emergency stop button is also connected to this device to disconnect the CAN bus from the CACC computer. Pressing this button gives full manual control to the driver.

Control Performance

The objective of the CACC system is to follow the lead vehicle at the specified reference distance. In this testing, the fuel savings results are quantified as a function of following distance. Therefore, analysis of the control system performance is important for understanding these results. Previously, Smith et al. [17] analyzed the same CACC system performance for a number of highway routes taken. The control performance is presented here to show the expected behavior in a more benign environment, a test track. The range estimate and controller error (range error) for a representative test case are shown in Figure 2. In the figure, the red line represents the input reference or set following distance. These results show the controller's ability to follow the lead vehicle at the given following distance. Over the entire test, the average and standard deviation of the error while platooning were 0.00 m and 0.34 m, respectively.

Manual Lateral Offset

Although longitudinal control is automated, steering control is maintained manually by the driver. During this test campaign, the effects of the lateral offset of platooning vehicles is investigated. A graphical user interface (GUI), shown in Figure 3, was developed as a driver visual aid. The GUI was designed to display an estimated lateral offset calculated on-line. The estimated lateral offset is derived from previous work shown in [20]. This approach uses a combination of precise GPS positioning techniques (Dynamic-base Real Time Kinematic and Time-Differenced Carrier Phase) and a Inertial Navigation System. These measurements are combined to form a relative path between lead and following vehicles. The lateral offset can then be calculated as shown in the "lateral offset calculation" section. The GUI was used to help maintain the desired offset in the straight sections of the track. In Figure 3, the colon (in the middle) represents the desired offset, or alignment, and each vertical bar represents 10 cm of error. For example, the figure below represents a lateral error between -30 and -40 cm, with a negative value represents an offset to the left relative to the lead vehicle. The two offset conditions used in this test are shown in Figure 4. The estimated lateral offset was calculated at 100 Hz and displayed on a tablet device mounted on the vehicle's dashboard, as shown in Figure 5. The location of the tablet was based on the drivers' preference to best use the GUI as a visual aid to keep the desired offset. In Figure 5, the tablet/GUI were being used for the max offset (1.3 m) test case at 9 m (30 ft) following distance.

Lateral Offset:

[---|||:------]

Figure 3: Estimated lateral offset for GUI application. 1 bar = 10 cm of lateral offset error to the reference.

Figure 4: Visual representation of the two offset conditions: left - half offset (0.65 m), right – max offset (1.3 m).

Figure 5: Example test case using the GUI displayed on the tablet (just above steering wheel) for the max offset test case.

Test setup and Procedures

Test Vehicles

Three class 8 heavy-duty tractors with 53-ft dry-van trailers were used as test vehicles in the fuel-economy study. Both lead and follower tractors were Peterbilt 579s (model year 2015), and the control truck was a Freightliner Cascadia (model year 2016). Trucks 1 (lead) and 2 (follower) are shown in Figure 6, and the control truck is shown in Figure 7. The SAE J1321 fuel consumption test procedure required identical vehicles to be used. In this study, however, the use of different tractor models for the test and control vehicles does not strictly conform to the SAE J1321 requirements. All tractors are aerodynamically treated with high roof fairings, chassis skirts, side extenders, and aerodynamic bumpers and were therefore expected to react similarly to changes in the environment that affect aerodynamic performance, particularly the ambient winds. More details about the test vehicles are presented in Table 1.

The trailers of all three vehicles were ballasted to provide a total vehicle mass of 29,500 kg (65,000 lb). The trailers were ballasted using concrete blocks aligned evenly along the centerline of the trailer. Fuel levels in the main tanks of the trucks were adjusted to match the weight amongst all three vehicles. For all tests, the trailers were outfitted with two aerodynamic technologies: side skirts (Transtex EDGE SKIRT 2330) and boat tails (Stemco TrailerTail Trident).

Figure 6: Photograph of Trucks 1 and 2 with 53-ft dry-van trailer and 9 m (30 ft) spacing.

Figure 7: Photograph of control truck with 53-ft dry-van trailer.

Table 1. Test Vehicle Specifications.

Specification	Leader	Follower	Control Truck
Name	Truck 1	Truck 2	Control Truck
Manufacturer	Peterbilt	Peterbilt	Freightliner
Model	579	579	Cascadia
Year	2015	2015	2016
Engine	Paccar MX-13	Cummins ISX15	Detroit DD15
Brake System	Bendix	Meritor WABCO	WABCO 4s/4m
Transmission	Eaton Fuller Automated 10 speed	Eaton Fuller Automated 10 speed	Detroit DT12-DA-1750
Trailer	Manac 53' Dry-van Trailer with	Manac 53' Dry-van Trailer with	Manac 53' Dry-van Trailer with

Specification	Leader	Follower	Control Truck
	Skirts and a Tail	Skirts and a Tail	Skirts and a Tail
Trailer Load	29,500 kg	29,500 kg	29,500 kg

Test Site

Testing was performed at the Transport Canada Motor Vehicle Test Centre operated by PMG Technologies in Blainville, Quebec, at 45.70 latitude and -73.87 longitude. The "Bravo" track was used for testing, which is a high-speed track with a primary surface of rain-grooved concrete. The track is a 6.5-km (4.0-mile)-long oval shape with two straight 1.6-km (1.0-mile) sections, and two 1.6-km (1.0-mile) constant-curvature banked sections. Figure 8 shows the level of curvature and bank, and Figure 9 shows an aerial view of the test track.

Figure 8: Trackside view of the test track showing a banked curved segment.

Figure 9: Aerial view of the test track; locations of track-side anemometers and truck refueling and staging are shown by yellow circles (adapted from Google Maps).

Measurements and Instrumentation

To understand the behavior of the tested vehicles better, a variety of parameters on each truck were measured and recorded using an imc® data acquisition system. Measurements included gravimetric fuel consumption, geographical position, on-board wind measurements, cooling flow measurements, engine-cooling performance, and driveshaft torque measurement, in addition to several variables from the vehicle network using CAN bus protocol. Geographical latitude and longitude of all trucks were recorded at a rate of 5 Hz using GPS antennas that were mounted on the roof of each tractor.

The gravimetric fuel economy measurements were undertaken using auxiliary fuel tanks with re-routing of fuel lines with quick-connect couplings. The auxiliary fuel tanks were mounted on the frame rails in the tractor-trailer gap as shown in Figure 10 and were exchanged by forklift between each measurement run. The fuel tanks were weighed using a precise scale with an accuracy of 0.02 kg that was verified periodically throughout the test campaign.

Track-side wind measurements were undertaken using sonic anemometers at mid-truck-height (approximately 2 m). A weather station, located approximately 100 m from the track at a height of 3.0 m (10 ft), acquired 10-second-mean environmental conditions for the site. In addition, the engine fuel rates and cruise control status were recorded from the vehicle network for all three trucks using the CAN bus protocol at a rate of 10 Hz.

Figure 10: Auxiliary fuel tanks mounted in the tractor-trailer gap.

Test Procedures

The fuel consumption measurements were performed according to the SAE J1321 Type II procedure [21]. This procedure is designed for evaluating changes in fuel economy pertaining to modifications to a vehicle. For the purpose of this test, the definition of "modification" has been extended to consider platooning as a modification to the aerodynamics shape of a vehicle.

For the baseline test segments, the three vehicles (two test vehicles + one control vehicle) were spaced approximately 2 km from each other during testing. For the truck-platoon tests, the control truck was spaced between 2 km and 3 km from the truck platoon. The trucks maintained a speed of 105 km/h (65 mph) for the duration of the test runs, using their respective cruise-control systems, with independent checks by a track-side radar located on the north-side straight segment of the track.

As noted earlier, the J1321 procedure requires the use of the same truck models and specifications, but the three vehicles were different. The J1321 procedure also requires the local winds to not exceed 20 km/h; however, some testing was completed with winds exceeding these limits. This test program is therefore not strictly valid as a J1321 result, but J1321has been used as a guide in this research effort.

Analysis Procedures

J1321 Gravimetric Fuel Consumption Analysis

The fuel-consumption data have been analyzed using the method described in the SAE J1321 Type II procedure [21]. The method was devised to minimize the influence of environmental and external factors that may change from run to run or from day to day. It makes use of fuel-use ratios between the test vehicles and the control vehicle, and relies on an assumption that the change in external factors affects the control vehicle in the same manner as the test vehicles. The ratio of test-vehicle fuel use (T) to the control-vehicle fuel use (C) is defined as:

$$T/C = \frac{m_{f,test}}{m_{f,control}} \quad (1)$$

where m_f represents the weight of the fuel consumed for the respective vehicle during a measurement run, as inferred through measurement of the fuel-tank weights before and after each test run. The fuel-savings measure is based on averages of the T/C ratios from the respective baseline runs and test runs and calculated according to:

$$\Delta F = \frac{\overline{(T/C)_{baseline}} - \overline{(T/C)_{test}}}{\overline{(T/C)_{baseline}}} \quad (2)$$

The data quality checks described in SAE J1321 [21] are performed by means of a comparative statistical analysis to define the validity of a measured ΔF value and assign an uncertainty value associated with a 95% confidence interval.

Data collected during this and other test programs have identified no measurable fuel savings for the lead vehicle for separation distances beyond about 25 m [5, 10, 14, 15]. For such cases, the lead vehicle is therefore experiencing conditions as if it was isolated from the other trucks and can therefore be considered a “control vehicle” for the trailing truck in the platoon arrangement. As a means of improving the quality of the measurements at these longer distances, fuel consumption data from the lead platoon vehicle have been used as the control data for the trailing truck at any test condition for which the separation distance was greater than 30 m (approximately 1 s time gap at 105 km/h). This approach improves accuracy by using a control vehicle of greater similarity (make and shape) to the test vehicle, and uses a control vehicle that is experiencing local environmental conditions of greater similarity to the test vehicle. As described by McAuliffe et al. [15], using the lead truck as the control vehicle for these scenarios, the calculated fuel-savings values of the following vehicles changed by no more than 1% using this approach, compared to using the control-truck data, but confidence intervals are often reduced by up to 1%, therefore providing improved accuracy of the measurements. The full-platoon results for these cases also make use of the lead vehicle as the control measure, while the lead-vehicle test results were calculated in the standard manner using the control vehicle as the control measure.

Track-Segment Analysis

The Bravo Track at the Motor Vehicle Test Centre has straight and curved segments as shown in Figure 9. A previous truck-platooning project on this track identified differences in the fuel savings associated with platooning between the straight and curved segments, with upwards of 5% higher fuel savings on the straight segments than on the curves [15]. For the current test program, a similar analysis was completed.

The J1321 gravimetric fuel-consumption results do not permit an assessment of the fuel use for different segments of the track, and therefore, an analysis of the fuel-rate signal broadcast by the vehicle through the J1939 CAN bus was undertaken. The J1939 CAN bus fuel-rate signals have been shown to differ from the true fuel use [10, 15] and therefore must be corrected for this analysis. The gravimetric fuel-weight measurements provide data against which the CAN bus fuel rate signals can be calibrated. This is accomplished by defining a scaling ratio between the measured fuel mass for each run, $m_{f,meas}$, and the integration of the CAN-bus volumetric-flow-rate signal over the duration of the test run, $V_{f,calc}$:

$$C_f = \frac{m_{f,meas}}{V_{f,calc}} = \frac{m_{f,meas}}{\int_{t,start}^{t,end} \dot{V}_f dt} \quad (3)$$

such that C_f is evaluated through linear regression based on nearly all the fuel measurements for the test campaign. Data points that differed from the linear trends by more than 5 standard deviations were eliminated from the analysis. The C_f values represent a combination of the CAN-bus fuel-rate offset and the density of the diesel fuel. Figure 11 shows the relationship between the measured and calculated fuel values and the regression fit for each of the three vehicles. For the purpose of the fuel-rate analysis, it is assumed that these calibration values apply equally well to the instantaneous fuel-rate signals as they do to the integrated signals, such that

$$\dot{m}_f = C_f \cdot \dot{V}_f \quad (4)$$

providing an indication of the mass flow rate of fuel at any instant during a test run.

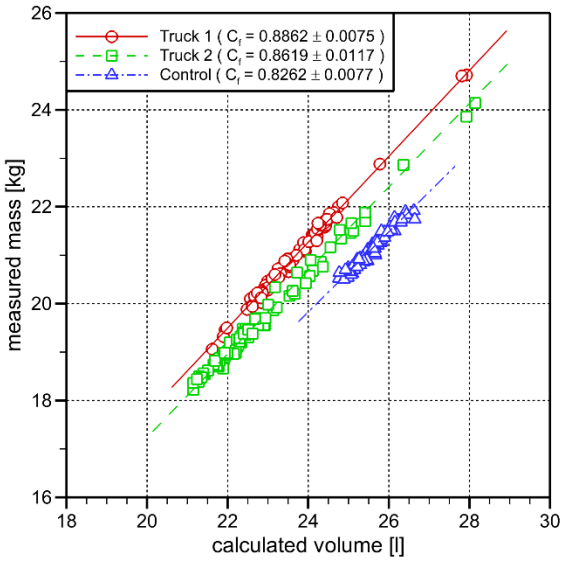

Figure 11: Linear regression results for the calibration of the J1939 CAN bus fuel-rate signals.

In Figure 11, Truck 2 demonstrates greater scatter in the data, resulting in a larger uncertainty in the fuel use estimates. These variations in scatter are likely due to the differing characteristics of the CAN-bus fuel-rate signals broadcast by the vehicles.

The CAN bus fuel-rate trends for Truck 1, Truck 2, and the Control Truck during single-truck baseline operation are shown in Figure 12. The eleven laps of CAN bus fuel-rate data are displayed as overlapping black traces, and the average CAN fuel-rate is overlaid in red. The disparate nature of the CAN fuel-rate data for the three trucks reflects the individual cruise control calibrations of the respective vehicles. Truck 1 and the Control Truck utilized their respective stock original equipment manufacturer ACC calibrations, while Truck 2 utilized a cruise control calibrated by the research team. Truck 1 demonstrates clean signals on the straight segments of the track, with significant variability in the curves. Truck 2 shows a noisy signal at all locations on the track with distinct low-frequency variations along the track. The control truck demonstrates the cleanest overall signals, but demonstrates a stepped signal caused by a low update rate or low reported resolution. All three vehicles demonstrate a drop in fuel rate mid-way along the south-side straight segment of the track. This is due to a change from positive grade in the first half (0.3 %) to a negative grade on the aft half (-0.25%) [22]. The north-side straight has a small negative grade of 0.05% that is consistent along the full stretch, except for a large sunk section near its end, which is the cause for the large negative spike in fuel rate for the control truck. Neither of the test trucks show a response to this sunk section of the north-side straight, indicating very different cruise control characteristics for each truck.

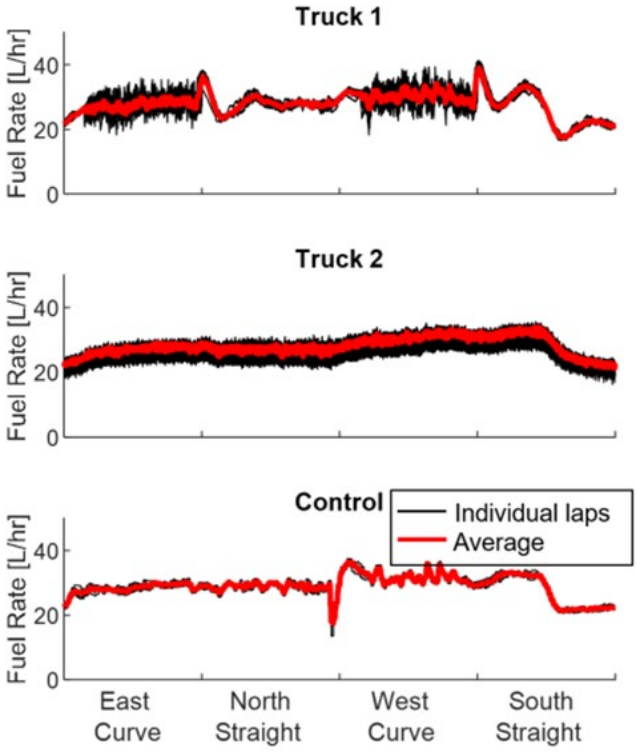

Figure 12: CAN bus fuel-rate characteristics for a baseline test run, excluding the first and last lap (11 laps shown, red line indicates the average of all laps).

The contrasting baseline CAN fuel-rate behavior of Trucks 1 and 2 is of particular interest. During platoon operation, Truck 2 utilizes the *"research team"* CACC system to follow Truck 1 at prescribed headway distances. Meanwhile, Truck 1 cruises at the desired speed utilizing its stock ACC system. Thus, the CAN fuel use rate of Truck 2 assumes a similar profile to Truck 1 during platooning operation, as shown in Figure 13. Note that the CAN fuel use rate perturbations in Truck 1 are not only assumed by Truck 2 during CACC operation, they are slightly exaggerated. It is hypothesized that unnecessary excitation of the fuel-rate profile reduces platoon fuel economy benefits. While the influence of these perturbations on the platooning fuel economy of Truck 2 is currently under investigation, the impact is outside the scope of the present study.

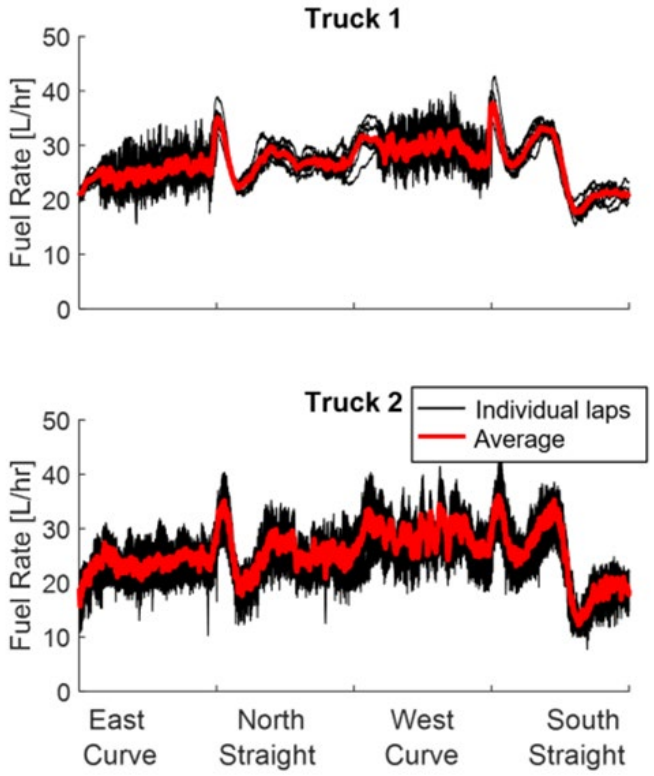

Figure 13: CAN bus fuel-rate characteristics for a platooning test run, excluding the first and last lap (11 laps shown, red line indicates the average of all laps).

The potential uncertainty in fuel-savings results associated with the fuel-rate calibrations has been evaluated by performing a J1321 analysis for a set of test runs using both the measured fuel-mass data and the corresponding calculated fuel-mass data, and comparing the results. This demonstrated an uncertainty on the fuel-savings results of 0.5% for Truck 1 results and 1.0% for Truck 2 results. All fuel-rate-analysis data presented in this paper have included this error as an independent error source, in addition to the confidence intervals calculated using a fuel-rate-based J1321 analysis procedure, described in the following paragraph.

A track-segmented fuel-savings analysis was performed using the same data analysis procedures as the SAE J1321 analysis. The track was broken down into four segments (east curve, north straight, west curve, south straight). The fuel used for each segment of each lap was calculated from the calibrated fuel-rate signals for each test run. A *T/C* value was then calculated for each segment in the following manner

$$T_i/_C\,(lap, segment) = \frac{C_{f,i}\int_{t,i,start}^{t,i,end}\dot{V}_{f,i}dt}{C_{f,C}\int_{t,C,start}^{t,C,end}\dot{V}_{f,C}dt} \quad (5)$$

where the subscripts *i* and *C* represent the vehicle of interest (1 or 2 for the test vehicle, C for the control vehicle). The fuel consumed for each segment within a lap was calculated based on the duration over which the respective vehicle was within the respective segment of the track. This approach introduces a difference in the absolute time limits for integration of data from each vehicle because they enter and exit each segment at different times. These time limits were identified using GPS position data. To provide a measure of consistency, data for the first and last laps of each test run were excluded from the analysis, to eliminate the acceleration and deceleration transients and thus provide data that represent steady-state driving conditions. This provides 44 data points (11 laps x 4 segments) per 13-lap test run. For some test configurations, large transients in fuel use were observed during a run, which were associated with either changes in the lead driver behavior or due to influences of the cruise control system of the lead truck. Any such transients that exceed approximately ±50% of the nominal fuel rate for a given location on the track (based on visual inspection of the fuel rate signals) were excluded from these analyses.

Lateral Offset Calculation

To further study the offset cases, a measure of the lateral offset is needed. As previously mentioned, an estimated value was displayed to help the driver maintain the offset. A more accurate method to obtain the "true" lateral offset is described here. The GPS unit on each vehicle logs the position and satellite range information at 2 Hz. At the end of a test, these binary GPS logs can be post-processed with real time kinematic (RTK) corrections to produce centimeter level accurate global positions [24]. These global positions are in the global Earth Centered Earth Fixed (ECEF), or XYZ, coordinate frame. These coordinates are then transformed to a local North East Down (NED) coordinate frame, using the staging location latitude, longitude, and altitude as the reference. The resulting GPS traces, shown in Figure 14, are used to calculate the lateral offset. In the figure, the blue points (x_1 , x_2) represent the lead vehicle's GPS coordinates, and the blue line is the path traveled. The red point represents a following vehicle's GPS waypoint and the lateral offset is calculated for each of these.

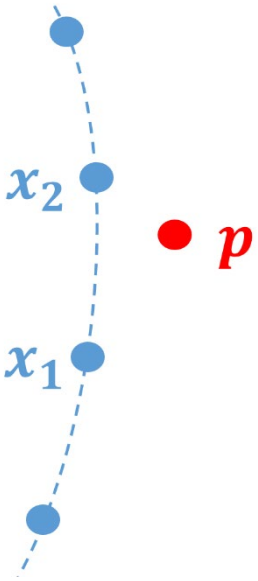

Figure 14: Example GPS waypoints for lead and following vehicles.

First, the closest lead vehicle GPS waypoint (to the following vehicle) must be determined. This is done by calculating the magnitude of distance for the lead vehicle's points near the point, p, and finding the minimum. Then, the lead vehicle's previous point is also selected. In Figure 14, point x_2 is calculated as the lead vehicle GPS point with the minimum distance to the point, and x_1 is the lead vehicle's previous point. These three points (x_1, x_2, p) now form a triangle, as shown in Figure 15a. The lateral error, e, is the magnitude of the projected line from point p to line segment, a, forming a right angle. Using geometry, the triangle is related by:

$$e = |c| * \sin\Theta \quad (6)$$

such that e is the lateral error, $|c|$ is the distance between points x_1 and p, and theta is the angle between line segment (x_1 , x_2) and point p. The angle theta can be calculated by the law of cosines:

$$\Theta = \cos^{-1}\left(\frac{a^2+c^2-b^2}{2ac}\right) \quad (7)$$

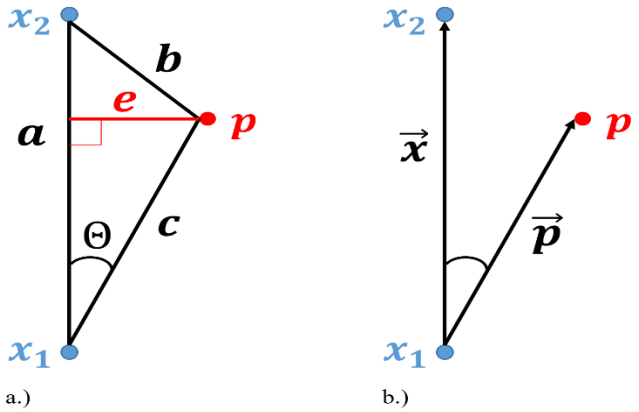

Figure 15a: Triangle formed by two lead vehicle GPS points and one following vehicle's. Figure 15b: Vectors formed to calculate the sign of lateral offset.

Next, two vectors are formed between the three points:

$$\vec{x} = \langle x_2 - x_1 \rangle \quad (8)$$
$$\vec{p} = \langle p - x_1 \rangle \quad (9)$$

These vectors are used to carry out the cross product. The cross product is needed to calculate the sign of the lateral offset value. The cross product is calculated as:

$$\vec{p} \times \vec{x} = \left(\vec{p}_E * \vec{x}_N\right) - \left(\vec{p}_N * \vec{x}_E\right) \quad (10)$$

where N and E represent the north and east components of the resulting vectors. This calculation does not include the Down component of the vector. Now the lateral offset can be calculated as:

$$e = sign(\vec{p} \times \vec{x}) * |c| * \sin\Theta \quad (11)$$

such that the sign of the cross product is taken. The resulting lateral offset has a negative or positive value representing offset to the left or right of the lead vehicle, respectively.

Manual Lateral Offset Performance

As previously stated, the lateral offset was controlled manually by the driver. In this testing, it is important to understand how well the offset was kept. The "true" lateral offset was calculated as described in the previous section, lateral offset calculation. Figure 16 shows the resulting lateral offset values for a representative test case at the Maximum Offset case of 1.3 m. It is important to note that the lateral offset was only kept in the straight segments of the track. The straight segments were extracted to analyze the manual lateral offset performance. The resulting average and standard deviation were -1.26 m and 0.15 m, respectively. These values represent the nominal lateral performance during the test campaign.

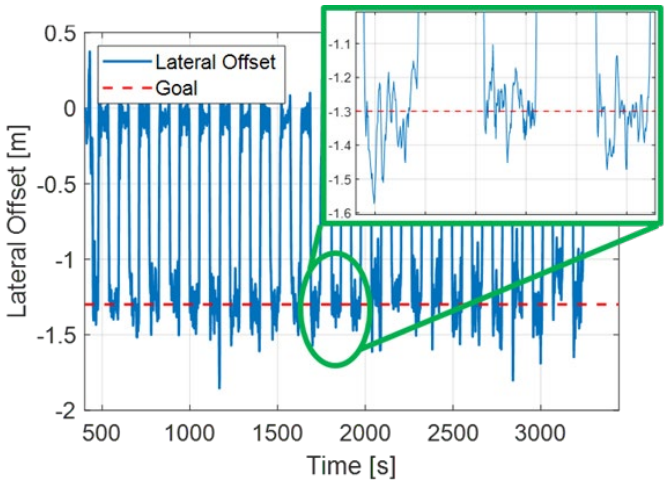

Figure 16: Calculated lateral offset for duration of a test run at the maximum offset.

Results

Aligned Platoon and Comparison to Past Results

To assess the sensitivity of truck platoons to unintentional driver misalignment, it was necessary to assess the performance of the system in the aligned position and compare the results to previously published studies with similar scenarios such as two-truck platoons at similar vehicle speed, mass, and separation distances. The studies selected [5, 10, 14, 15] all had tests run at 65 mph and 65,000 lbs using North American Class 8 trucks over an overlapping range of following distances. All tests included trailers with side skirts, and all but one [10] used trailer tails. All but one test series [5] tested two-truck platoons; for that exception, the middle truck in a three-truck platoon was used to represent the trailing truck of the two-truck platoon when the third truck was at distances greater than 20 m, for which the presence of the third vehicle should not impact reported savings of the middle truck. In Figures 17 and 18, the four selected studies are combined into the average, minimum, and maximum grey lines for lead and trailing trucks by adding or subtracting the published 95% confidence intervals to the value at each following distance. Because not all tests shared all following-distance test points, some distances have more data included. The intention is to provide the reader with the range of previously reported truck platooning results in a clear manner.

Figure 17 shows how the lead and trailing trucks in the current work compare to the previous studies. Both trucks generally demonstrated 1%–2% higher savings than the average of the previous studies at distances less than 46 m (150 ft). At most points, the confidence intervals of the new work are bounded by the maximum of the previous studies, indicating that the range of possible results includes a common answer (the exception is the 30-ft case for the lead truck). Both the lead and trailing trucks demonstrate the previously established savings trends, quickly increasing savings for the lead vehicle at distances less than 15 m (50 ft) and savings for the trailing vehicle steadily increasing to a maximum at about 12 to 15 m (40 to 50 ft) followed by reduced savings at closer distances.

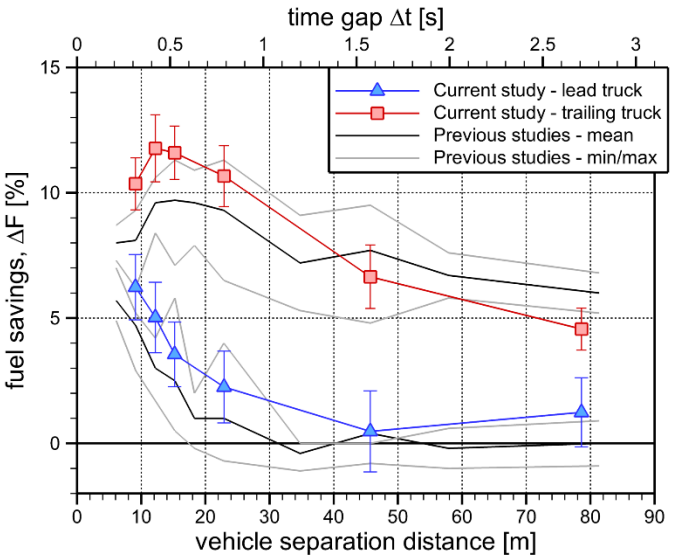

Figure 17: Current individual truck savings compared to past results.

Figure 18 shows how the truck platoon fuel savings considered as a team in the current work compares to the previous studies. This more clearly highlights that while there is significant overlap, the current study produced results that are nominally lower than past studies at long following distances and nominally higher in the close following scenarios. It is not known at this time what combination of tractor aerodynamics, ambient conditions, and controls may be responsible for this difference.

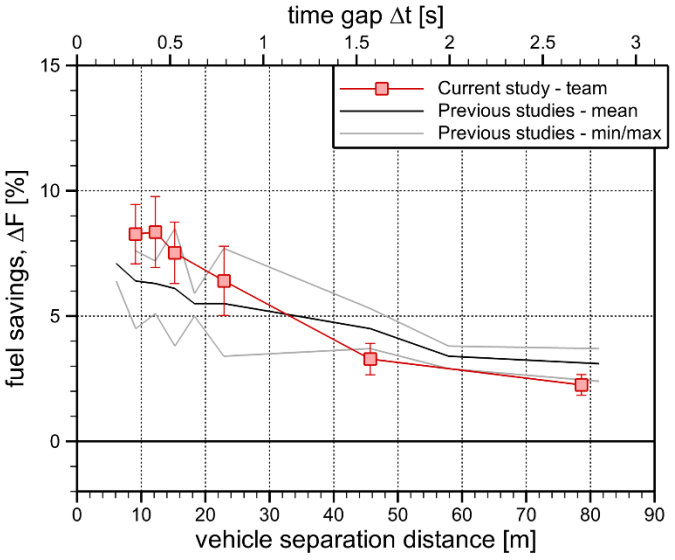

Figure 18: Current platooning team savings compared to past results

J1939 CAN bus Track-Segment Results

For the aligned platoon, Figure 19 compares the test results of the J1321 gravimetric fuel-savings analysis to that the equivalent analysis using the track-segmented CAN bus fuel-rate approach. For many of the data points, the confidence intervals associated with the CAN-bus fuel-rate results are smaller than those for the gravimetric analysis. This is a result of having many more data points with which to calculate the uncertainty of these measurements (upwards of 33 data points for three test runs) compared to the gravimetric analysis (three data points for three test runs). The CAN bus fuel rate confidence intervals have been calculated to include the influence of calibration uncertainty in addition to the statistically defined uncertainty due to the variance of the data points.

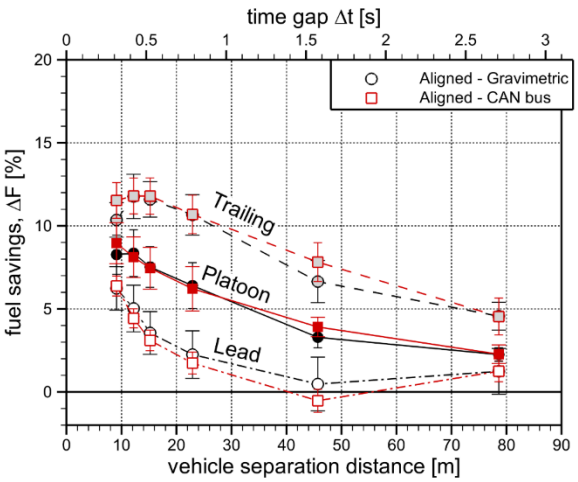

Figure 19: Comparison between the fuel economy results using the calibrated CAN bus fuel-rate signal and the gravimetric procedure for the aligned platoon.

Some differences on the order of 1% fuel savings or greater are observed in the test results between the two analysis methods in Figure 19, most apparently at separation distances of 9 m (Truck 2) and 46 m (both trucks), although all differences are within the respective confidence intervals. For Truck 2 at 9 m separation, the differences are attributed mainly to the elimination of large transients in fuel use during the acceleration period and some mid-run transient behavior associated with the lead truck's cruise control system. The full-platoon fuel-savings data based on the CAN-bus fuel-rate analysis recover the expected trend of a monotonically decreasing fuel savings with separation distance as observed in other truck-platooning studies shown in Figure 18. At 46-m separation, the differences arise due to the absence of CAN-bus data for two of the three test runs, and therefore the gravimetric data represent a larger range of test conditions.

Of particular note in Figure 19 is the persistence in the positive fuel savings for Truck 1 at 78 m separation distance. Unlike the gravimetric data, for which the confidence interval straddles zero, the CAN bus fuel-rate analysis shows a distinctive fuel savings at this condition. This may be due to largely different wind conditions encountered for this test condition (strong easterly and southeasterly winds), compared to the baseline test runs (predominantly south and southwesterly winds).

With the verification based on Figure 19 that the CAN-bus fuel-rate data can be applied with the J1321 fuel-savings-analysis procedures, the fuel rate data were interrogated to identify the fuel savings for each segment of the test track (east curve, north straight, west curve, south straight), from which the differences in curved versus straight track segments have been evaluated. Figure 20 shows the differences in platoon fuel savings between the straight and curved segments of the track compared to the track-averaged results. The lead truck shows no measurable difference between the straight and curved segments, whereas Truck 2 shows a 6% difference at the shortest separation distances and 10% difference at the largest separation distance, with larger fuel savings on the straight segments.

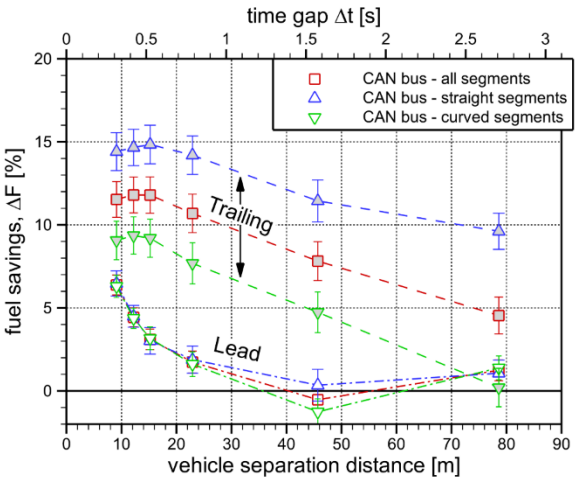

Figure 20: Comparison of the fuel savings of the aligned platoon for the straight and curved segments of the track to those of the full track.

These evaluations are based on percentage changes in fuel use on each segment; therefore, a decrease in platooning fuel savings in the curves of the track may be attributed to either an increase in the baseline fuel use or a decrease in fuel savings use during the test runs. Figure 21 shows the fuel-use split amongst the four segments of the track based on a series of five baseline runs. It is evident that the net fuel use trends are similar for each of the three vehicles despite the varied instantaneous fuel-rate characteristics shown earlier in Figure 12. The fuel-use split clearly shows an increased fuel use in the curves, with more fuel used in the west curve than the east curve, which can be attributed to different grades (2-m elevation increase in the west curve versus 1-m elevation decrease in the east curve). Despite the differences in grade characteristics between the north and south straight segments, they each contribute almost equally to the fuel use along the track.

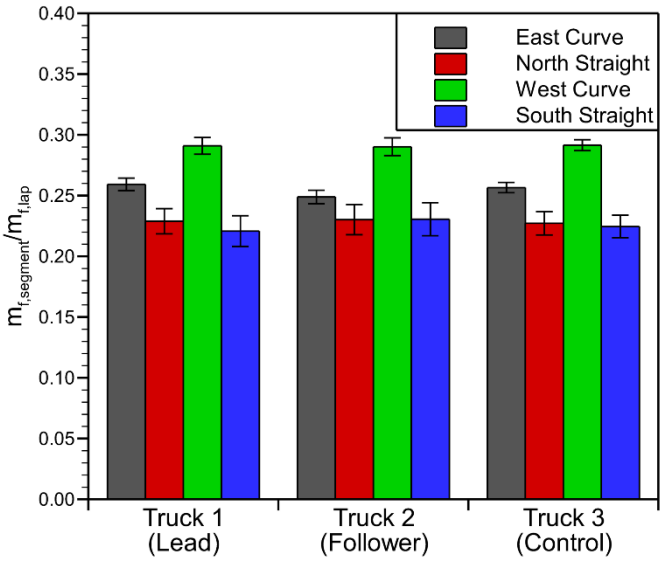

Figure 21: Fuel use split amongst the four segments of the test track.

The fuel use characteristics in Figure 21 show that, of the total fuel used per lap, approximately 55% is used in the curves and 45% in the straights. If platooning fuel savings (absolute magnitude) were constant in the curves and straights, it would contribute to about 1% increase in fuel use on the straights and 1% decrease on the curves, when calculated as a percentage like the data of Figure 20, due to the changes in the denominator of the equation. Given the much larger differences shown in Figure 20, it can therefore be inferred that the platooning benefit is degraded in the curved sections of the track. This implies that platooning may achieve greater benefits for predominantly straight roadways, although the general sensitivity to curvature cannot be gauged by the current study due to the single road-curvature condition encountered.

A contributing factor for the change in fuel-use characteristics amongst the straight and curved track segments is likely the misaligned articulation of the tractor and trailer when traveling in a curve. This effect has been highlighted by Ellis and Mihelic [23] as a potential source of discrepancy between track testing and other aerodynamic evaluation techniques, such as wind tunnel or simulation approaches. They identified an increase in aerodynamic drag in excess of 10% for three degrees of articulation, representing a radius of curvature of about 250 m (approximately half what is experienced in the current study). This is likely one possible source of the increased fuel use in the curves, as identified in Figure 21. Furthermore, the articulation may impact the wake structure behind the vehicle and the associated platooning benefits of a trailing vehicle.

In Figure 20, the lead vehicle exhibits no change in fuel savings between the straight and curved segments of the track. Given the increased fuel use in the banks, it is currently unclear the reason for the similarity in fuel savings for this lead truck.

The differences between curved and straight segments observed in this study are greater than those observed by McAuliffe et al. [15] for the three-truck platoon previously tested at the same test track. In that study, the control vehicle did not broadcast its instantaneous fuel rate, and an assumption was made that the fuel rates for the baseline cases were equal for each segment of the track, which, based on the results of the current study (Figure 21), is likely not the case. If the straight-versus-curved fuel-use split of Figure 21 can be assumed to apply to the previous test campaign, then a greater difference would be expected in the associated platoon savings, in the same manner observed in the current data set. It should be emphasized that the curved segments of this track are not representative of standard curved roadways. The banked surface provides different conditions for the track than would be encountered on standard highways, as shown in Figure 8.

Influence of Lateral Offset

To evaluate the sensitivity of fuel savings to lateral alignment, testing was undertaken at two magnitudes of lateral offset, each of which was evaluated at the four smallest separation distances (up to 23 m). The maximum offset case was defined based on the maximum lateral offset used by Salari and Ortega [3] in their wind-tunnel test program, representing half a truck width (1.3 m). The half-offset case represents a quarter-truck-width offset (0.65 m). The drivers were instructed to maintain the offset on the straight segments of the track, while returning to aligned formation in the banked curve to prevent lateral forcing of the vehicles from their neutral position on the curve.

Figure 22 shows the J1321 gravimetric fuel-savings results for the aligned and offset cases. Most of the offset cases show a decrease in platooning benefit for both vehicles; however, there are no apparent trends related to the magnitude of the offset. It might be expected that the fuel savings reduces monotonically with offset, but this is not observed in the current results.

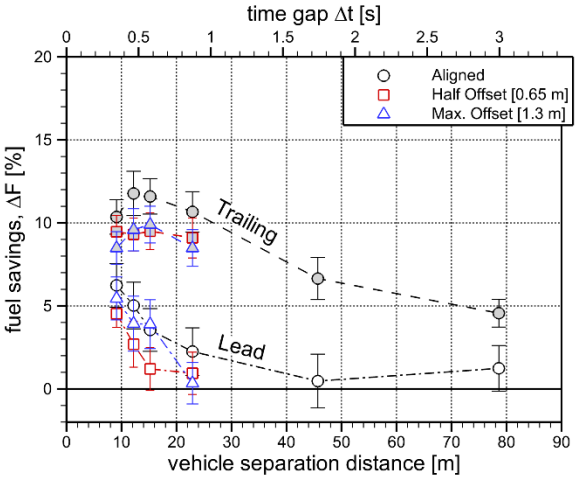

Figure 22: Fuel savings results of the aligned and lateral-offset cases, based on the gravimetric fuel analysis.

The impetus for implementing the CAN-bus-based fuel-savings analysis was to examine the offset effects only when the trucks were offset on the straight segments of the track. This analysis is also helpful to identify the source of the conflicting trends between the half- and maximum-offset results. By offsetting the platoon only on the straight segments, the curved segments should show no difference between the aligned-platoon and offset-platoon tests. As shown in Figure 23, this is not the case. On the curves, the trailing truck shows small variability in the fuel savings amongst the cases, all within the experimental uncertainty. The lead vehicle, however, shows a distinct difference between the maximum offset case and the aligned case, indicating that some additional variable is affecting the test results. This additional variable is likely the wind, as discussed in the next paragraph.

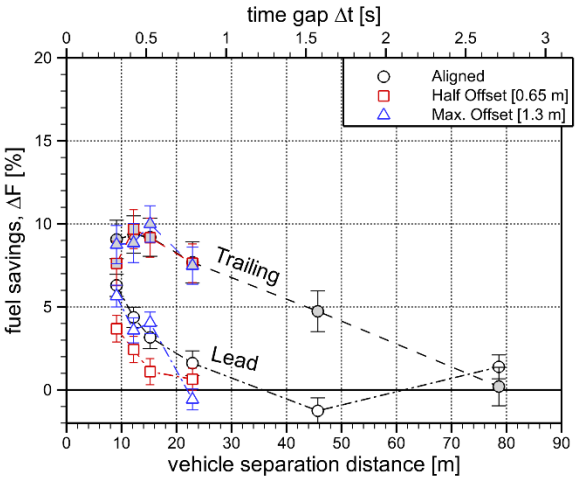

Figure 23: Fuel savings results of the aligned and lateral-offset cases for the curved segments of the track, based on the CAN-bus fuel-rate analysis.

The wind constraints imposed by the J1321 procedure were relaxed during the current test program, resulting in testing during conditions with winds exceeding the 20 km/h threshold for J1321 validity. All of the half-offset test cases experienced wind exceeding this threshold, while only one of each of the aligned or maximum-offset cases

experienced a brief period with excessive winds. As an example of the differing wind conditions, Figure 24 presents aggregate wind roses for the aligned, half-offset, and maximum-offset cases at a separation distance of 15 m (50 ft). The baseline, aligned-platoon, and maximum-offset cases show a small proportion of, or no occurrence of, wind speeds above 10 km/h (mostly shades of blue), while the half-offset case shows a large majority of winds speeds exceeding 10 km/h (mostly green, orange and red). Furthermore, the high winds for the half-offset case are predominantly cross-winds relative to the straight segments of the track for which the offset test were undertaken. These wind results suggest that a comparison of the half-offset test data to the aligned or maximum-offset data may not be reliable. The 12 m (40 ft) and 23 m (75 ft) half-offset cases experienced similar wind conditions to the 15 m (50 ft) case identified in Figure 24, with these representing the highest sustained wind conditions experienced through the test campaign. The 9 m (30 ft) half-offset case experienced similar wind magnitudes to these cases, but with the predominant direction aligned with the straight segments of the track.

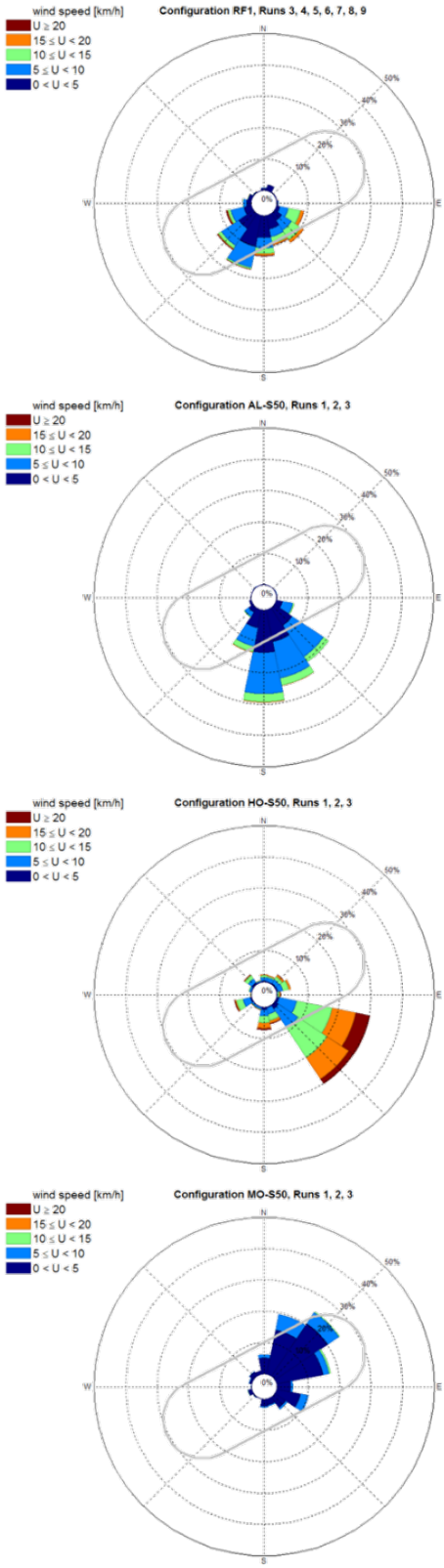

Figure 24: Aggregate wind conditions from the on-site weather station for the baseline runs (top), aligned 15-m platoon runs (second from top), half-offset 15-m platoon runs (second from bottom), and maximum-offset 15-m platoon runs (bottom). The track orientation is shown as a grey line overlaid on each wind rose.

With the wind conditions providing context for comparing the offset-platoon cases to the aligned-platoon cases, the maximum-offset data

are likely a more reliable estimate of the potential fuel savings when driving in the respective offset condition than are the half-offset test data. Figure 25 shows the calculated fuel savings for the straight segments of the track for the aligned and offset cases. The maximum offset data suggest that there is no significant impact on fuel savings of the lead vehicle when offsetting the platoon. At maximum offset, the trailing vehicle demonstrated approximately 3% to 4% reduction in fuel savings due to the offset. Although this is a measurable change in fuel savings, it represents only a portion of the savings while aligned and can be considered a maximum reduction possible, given that this offset condition creates a platoon that exceeds typical lane widths (3.9-m total width at maximum offset, compared to 3.7-m typical lane widths). The wind-tunnel experiments of Salari and Ortega [3] show increases in wind-averaged drag coefficient in excess of 6% of the aligned-platoon values when offset to half a truck width (1.3 m full scale). If aerodynamic drag is estimated to be 50% of the overall road load, then this would translate to at least 3% reduction in fuel savings, which is consistent with the current study. Of particular note in the data of Salari and Ortega [3], as well as in the wind-tunnel data of McAuliffe and Ahmadi-Baloutaki [4], the sensitivity of aerodynamic drag-benefit to lateral offset is much less when considering the offsets that might feasibly be experienced within a typical lane width (offset up to about 0.8 m). These combined studies therefore suggest that lateral offset control may not have a sizeable impact on fuel savings, although it has other benefits such as reduced driver workload, and possibly reduced cooling-flow impacts, neither of which is discussed in the context of this paper.

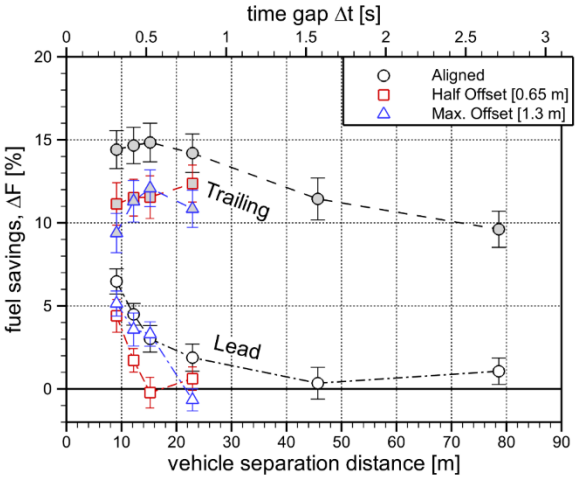

Figure 25: Fuel savings results of the aligned and lateral-offset cases for the straight segments of the track, based on the CAN-bus fuel-rate analysis.

The straight-segment data in Figure 25 can be further divided between the north-side and south-side straight segment of the track. These data are presented in Figure 26, which shows a further difference in fuel savings. The trailing vehicle of the aligned platoon experiences approximately 3% greater fuel savings on the south-side straight segment than on the north-side segment. This is perhaps due to the different grade profiles on each of these segments, combined with the changes in fuel-rate characteristics for Truck 2 when in platoon formation (contrast Figure 13 with Figure 12, discussed earlier). These data suggest that small grade changes along a straight roadway may degrade the potential benefits of truck platooning, but this influence will likely be dependent on the implementation of the control strategy.

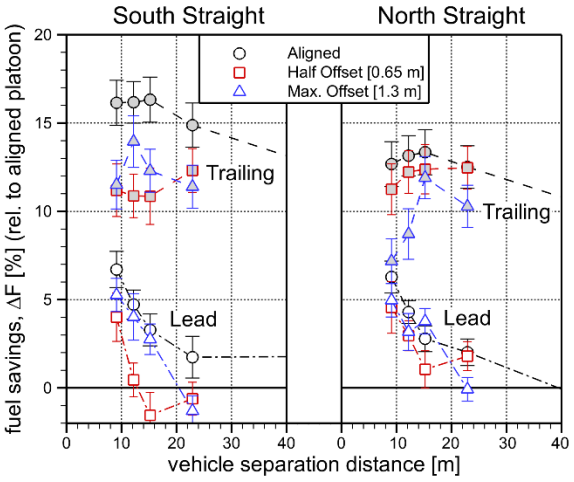

Figure 26: Fuel savings results of the aligned and lateral-offset cases for the south-side and north-side straight segments of the track based on the CAN-bus fuel-rate analysis.

Examining the offset test cases of Figure 26, the north-side data show trends that one might expect from the offset test cases, unlike the south-side in the same figure or full-lap data of Figure 23. For the north-side straight, the half-offset results for the lead vehicle show similar fuel savings to the aligned and maximum offset cases, and the trailing vehicle exhibits fuel savings between those of the aligned and maximum offset cases. The differences between the north-side and south-side straights may be influenced by a combination of the different grade profiles and the manner in which near-ground winds are sheltered differently by the local forest vegetation on either side of the track.

Summary/Conclusions

The results reported here represent a new assessment of a possible factor influencing the energy savings of truck-platooning systems. The fuel consumption for each truck of a two-truck platoon was measured using the SAE J1321 Type II procedure while travelling at 105 km/h (65 mph) and loaded to a gross weight of 29,500 kg (65,000 lb). Deviations from the standard J1321 procedures include the use of different test and control vehicles, and the exceedance of wind limits for some test cases. Vehicle separations ranging from 2.7 to 0.32 s (79 to 9 m) were tested for an aligned platoon, while multiple lateral offsets (0.65 m and 1.3 m) were tested over the range of 0.79 to 0.32 s (23 to 9 m). A calibrated J1939 fuel consumption analysis was completed to enable a track-segment analysis of platoon savings. Significant findings include:

- The previously established truck platooning savings trends continue to generally hold regardless of specific tractor aerodynamics, test track specifics, and control algorithm differences.
- Truck platoon savings on relatively straight public highways have the potential to exceed official SAE J1321 results as track segment analysis shows higher achieved savings on the straight track sections than the test as a whole. Based on the current results, exceedances of 3% to 4% savings over previously published results may be realized.
- The lateral offsets investigated for the following truck (0.65 m and 1.3 m) have a measurable negative impact on observed fuel savings (3% to 4% observed at the maximum offset when straddling the adjacent lane), but small unintentional driver

offsets during every-day driving are not expected to have a measurable impact on fuel savings.

- Realized truck platoon savings will be impacted by crosswind conditions but not negated.

- The track-segmented fuel-rate analysis introduced in the paper, based on calibrated J1939 fuel-rate signals, has been demonstrated to provide results consistent with the SAE J1321 gravimetric method, while providing the opportunity to analyzing data for individual segments of each test run and retaining similar levels of experimental accuracy.

References

1. Marcu, B., and Browand, F., "Aerodynamic Forces Experienced by a 3-Vehicle Platoon in a Crosswind," SAE Technical Paper 1999-01-1324, 1999.
2. Tsuei, L., and Savas, O., "Transient Aerodynamics of Vehicle Platoons during in-line Oscillations," *Journal of Wind Engineering and Industrial Aerodynamics* 89:1085-1111, 2001.
3. Salari, K., and Ortega, J., "Experimental Investigation of the Aerodynamic Benefits of Truck Platooning," SAE Technical Paper 2018-01-0732, 2018, https://doi.org/10.4271/2018-01-0732.
4. McAuliffe, B., and Ahmadi-Baloutaki, M., "A Wind-Tunnel Investigation of the Influence of Separation Distance, Lateral Stagger, and Trailer Configuration on the Drag-Reduction Potential of a Two-Truck Platoon," *SAE Int. J. Commer. Veh.* 11(2):125–150, 2018, doi:10.4271/02-11-02-0011.
5. McAuliffe, B.R., Ahmadi-Baloutaki, M., Croken, M., and Raeesi, A., "Fuel-Economy Testing of a Three-Vehicle Truck Platooning System," NRC Report LTR-AL-2017-0008, National Research Council Canada, 2017.
6. Bonnet, C., and Fritz, H., "Fuel Consumption Reduction in a Platoon: Experimental Results with Two Electronically Coupled Trucks at Close Spacing," SAE Technical Paper 2013-01-0767, 2000.
7. Browand, F., McArthur, J., and Radovich, C., "Fuel Saving Achieved in the Field Test of Two Tandem Trucks," California PATH Research Report UCB-ITSPRR-2004-20, 2004.
8. Al Alam, A., Gattami, A., and Johansson, K., "An Experimental Study on the Fuel Reduction Potential of Heavy Duty Vehicle Platooning," In 13th International IEEE Annual Conference on Intelligent Transportation Systems, Madeira Island, Portugal, 2010.
9. Roeth, M., "CR England Peloton Technology Platooning Test Nov. 2013," North American Council for Freight Efficiency (NACFE), Peloton, 2013.
10. Lammert, M., Duran, A., Diez, J., Burton, K., et al., "Effect of Platooning on Fuel Consumption of Class 8 Vehicles Over a Range of Speeds, Following Distances, and Mass," *SAE Int. J. Commer. Veh.* 7(2), 2014, doi:10.4271/2014-01-2438.
11. Tsugawa, S., "Results and Issues of an Automated Truck Platoon within the Energy ITS Project," In 2014 IEEE Intelligent Vehicles Symposium (IV), June 8-11, Dearborn, MI, 2014.
12. Humphreys, H. and Bevly, D., "Computational Fluid Dynamic Analysis of a Generic 2 Truck Platoon," SAE Technical Paper 2016-01-8008, 2016, https://doi.org/10.4271/2016-01-8008.
13. Roberts, J., Mihelic, R., Roeth, M., and Rondini, D., "Confidence Report on Two-Truck Platooning," Technical Report, North American Council for Freight Efficiency, 2016.
14. Bevly, D., Murray, C., Lim, A., Turochy, R., et al., "Heavy Truck Cooperative Adaptive Cruise Control: Evaluation, Testing, and Stakeholder Engagement for Near Term Deployment: Phase Two Final Report," Technical report, Auburn University, 2017.
15. McAuliffe, B., Lammert, M., Lu, X.-Y., Shladover, S.E., et al., "Influences on Energy Savings of Heavy Trucks Using Cooperative Adaptive Cruise Control," SAE WCX18 2018-01-1181, April 2018.
16. McAuliffe, B., Raeesi, A., Lammert, M., Smith, P., Hoffman, M., Bevly, D., "Impact of Mixed Traffic on the Energy Savings of a Truck Platoon," SAE WCX20 2020-01-0679, April 2020
17. Smith, P. and Bevly, D., "Analysis of On-Road Highway Testing for a Two Truck Cooperative Adaptive Cruise Control (CACC) Platoon," SAE Technical Paper 2020-01-5009, 2020.
18. Smith, P., Ward, J., Pierce, J., Bevly, D., and Daily, R., "Experimental Results and Analysis of a Longitudinal Controlled Cooperative Adaptive Cruise Control (CACC) Truck Platoon," Dynamic Systems and Control Conference, 2019.
19. Quigley, M., Gerkey, B. P., Conley, K., Faust, J., et al., "ROS: An open-source Robot Operating System," ICRA Workshop on Open Source Software. 3. 1-6, 2009.
20. W. Travis, "Path Duplication using GPS Carrier Based Relative Position for Automated Ground Vehicle Convoys," Ph.D. dissertation, Auburn University, Auburn, Alabama, 2010.
21. SAE J1321, "Fuel Consumption Test Procedure - Type II," Surface Vehicle Recommended Practice J1321, 2012.
22. McAuliffe, B., and Chuang, D., "Coast-down and Constant-speed Testing of a Tractor-trailer Combination in Support of Regulatory Developments for Greenhouse Gas Emissions," NRC Report LTR-AL-2016-0019-R, National Research Council Canada, 2016.
23. Mihelic, R., and Ellis, M., "Ramifications of Test Track Curves on Aerodynamic Prediction for Tractor Trailer Vehicles," SAE Paper 2013-01-2460, 2013.
24. Misra, P., and Enge, P. "Global Positioning System: Signals, Measurements, and Performance," (Lincoln, MA: Ganga-Jamuna Press, 2011).

Contact Information

Michael Lammert
michael.lammert@nrel.gov
National Renewable Energy Laboratory
15013 Denver West Parkway
Golden, CO 80401
(303) 275-4067
ORCID: 0000-0002-5888-7594

Brian McAuliffe
Brian.McAuliffe@nrc-cnrc.gc.ca
National Research Council Canada
1200 Montreal Road, Building M-2
Ottawa, Ontario, Canada K1A0R6
(613) 998-9201

David M. Bevly
dmbevly@eng.auburn.edu
1418 Wiggins Hall
Auburn University
Auburn, AL 36849
(334) 844-3446

Acknowledgments

This work was authored in part by the National Renewable Energy Laboratory, operated by Alliance for Sustainable Energy, LLC, for the U.S. Department of Energy (DOE) under Contract No. DE-AC36-08GO28308. Support for the work was also provided by the U.S. Department of Transportation (DOT) - Federal Highway

Administration under Agreement IAG-19-02109. The views expressed in the article do not necessarily represent the views of the DOE, DOT or the U.S. Government. The U.S. Government retains and the publisher, by accepting the article for publication, acknowledges that the U.S. Government retains a nonexclusive, paid-up, irrevocable, worldwide license to publish or reproduce the published form of this work, or allow others to do so, for U.S. Government purposes.

The work by the researchers from the National Research Council Canada was funded by Transport Canada's ecoTECHNOLOGY for Vehicles program. The views and opinions of authors expressed herein do not necessarily state or reflect those of Transport Canada.

The work by researchers from Auburn University was funded by the U.S. Department of Transportation - Federal Highway Administration under contract No. DTFH61-13-H-00019.

The authors would like to thank the staff from all the organizations that provided support to the project, including:

- Transport Canada Innovation Centre, with project oversight by Marc Belzile and Pierre Villemure, and with track support led by Dominique-Pierre Dion
- NRC project management by David Poisson, with track support by David Chuang, Mark Croken, and Sheldon Harrison
- Auburn University GPS \& Vehicle Dynamics Laboratory, with contributions of Jacob Ward, Evan Stegner, Christian Campos-Vega, and Dan Pierce
- FP Innovations PIT group, with track support led by Steve Mercier
- PMG Technologies, with track support led by Claude Sauvageau and Gilles Marleau
- Drivers supplied by Centre de Formation du Transport Routier de Saint-Jérome

Definitions/Abbreviations

CACC	Cooperative Adaptive Cruise Control
CAN	Controller Area Network
DSRC	Dedicated Short Range Communications
GPS	Global Positioning System
GUI	Graphical User Interface

Appendix

The fuel-savings results from the test campaign are provided in Tables A.1 through A.4. The J1321 gravimetric results are presented in Table A.1. The CAN-bus fuel-rate results for the full track, the straight segments, and the curved segments are presented in Tables A.2, A.3, and A.4, respectively.

Table A.1. Results from the SAE J1321 gravimetric fuel-consumption tests. The data represent vehicle speeds of 105 km/h (65 mph) and vehicle masses of 29,500 kg (65,000 lb).

Test Configuration	Separation Time [s]	Separation Distance [m]	Lead Truck Fuel Savings [%]	Trailing Truck Fuel Savings [%]	Platoon Fuel Savings [%]
Aligned	0.32	9.1	6.2 ± 1.3	10.4 ± 1.0	8.3 ± 1.7
	0.42	12.2	5.0 ± 1.4	11.8 ± 1.3	8.4 ± 1.9
	0.53	15.2	3.6 ± 1.3	11.6 ± 1.1	7.6 ± 1.7
	0.79	22.9	2.3 ± 1.4	10.7 ± 1.2	6.5 ± 1.9
	1.58	45.7	0.5 ± 1.6	6.6 ± 1.3	3.3 ± 0.6
	2.71	78.6	1.2 ± 1.4	4.6 ± 0.8	2.3 ± 0.4
0.65 m Lateral Offset	0.32	9.1	4.5 ± 0.8	9.5 ± 1.0	7.0 ± 1.3
	0.42	12.2	2.7 ± 1.4	9.3 ± 1.0	6.0 ± 1.7
	0.53	15.2	1.2 ± 1.3	9.5 ± 1.1	5.4 ± 1.7
	0.79	22.9	0.9 ± 1.3	9.1 ± 1.2	5.0 ± 1.8
1.3 m Lateral Offset	0.32	9.1	5.4 ± 1.3	8.5 ± 1.0	7.0 ± 1.6
	0.42	12.2	3.9 ± 1.7	9.6 ± 1.3	6.8 ± 2.1
	0.53	15.2	3.9 ± 1.5	9.9 ± 1.1	6.9 ± 1.8
	0.79	22.9	0.3 ± 1.3	8.5 ± 1.1	4.4 ± 1.7

Table A.2. Results from the CAN-bus fuel-rate analysis for the full track. The data represent vehicle speeds of 105 km/h (65 mph) and vehicle masses of 29,500 kg (65,000 lb).

Test Configuration	Separation Time [s]	Separation Distance [m]	Lead Truck Fuel Savings [%]	Trailing Truck Fuel Savings [%]	Platoon Fuel Savings [%]
Aligned	0.32	9.1	6.4 ± 0.6	11.5 ± 1.1	9.0 ± 1.2
	0.42	12.2	4.4 ± 0.6	11.8 ± 1.1	8.1 ± 1.2
	0.53	15.2	3.1 ± 0.6	11.8 ± 1.1	7.4 ± 1.3
	0.79	22.9	1.7 ± 0.7	10.7 ± 1.2	6.2 ± 1.3
	1.58	45.7	-0.5 ± 0.7	7.8 ± 1.2	3.9 ± 0.6
	2.71	78.6	1.2 ± 0.6	4.5 ± 1.1	2.3 ± 0.6
0.65 m Lateral Offset	0.32	9.1	4.0 ± 0.7	9.2 ± 1.2	6.6 ± 1.4
	0.42	12.2	2.1 ± 0.6	10.5 ± 1.1	6.3 ± 1.3
	0.53	15.2	0.5 ± 0.7	10.3 ± 1.1	5.4 ± 1.3
	0.79	22.9	0.6 ± 0.6	9.8 ± 1.1	5.2 ± 1.2
1.3 m Lateral Offset	0.32	9.1	5.4 ± 0.6	9.0 ± 1.1	7.2 ± 1.3
	0.42	12.2	3.6 ± 0.7	10.0 ± 1.1	6.8 ± 1.3
	0.53	15.2	3.7 ± 0.6	11.0 ± 1.1	7.3 ± 1.2
	0.79	22.9	-0.6 ± 0.6	9.0 ± 1.1	4.2 ± 1.2

Table A.3. Results from the CAN-bus fuel-rate analysis for the straight track segments. The data represent vehicle speeds of 105 km/h (65 mph) and vehicle masses of 29,500 kg (65,000 lb).

Test Configuration	Separation Time [s]	Separation Distance [m]	Lead Truck Savings [%]	Trailing Truck Fuel Savings [%]	Platoon Fuel Savings [%]
Aligned	0.32	9.1	6.5 ± 0.8	14.4 ± 1.1	10.4 ± 1.4
	0.42	12.2	4.5 ± 0.7	14.7 ± 1.1	9.6 ± 1.3
	0.53	15.2	3.0 ± 0.8	14.8 ± 1.2	8.9 ± 1.4
	0.79	22.9	1.9 ± 0.8	14.2 ± 1.2	8.0 ± 1.4
	1.58	45.7	0.3 ± 1.0	11.4 ± 1.3	5.7 ± 0.6
	2.71	78.6	1.1 ± 0.8	9.6 ± 1.1	4.8 ± 0.5
0.65 m Lateral Offset	0.32	9.1	4.4 ± 1.0	11.1 ± 1.3	7.8 ± 1.6
	0.42	12.2	1.7 ± 0.7	11.5 ± 1.1	6.6 ± 1.3
	0.53	15.2	-0.2 ± 0.9	11.6 ± 1.3	5.7 ± 1.6
	0.79	22.9	0.6 ± 0.7	12.4 ± 1.1	6.5 ± 1.3
1.3 m Lateral Offset	0.32	9.1	5.1 ± 0.8	9.4 ± 1.2	7.3 ± 1.4
	0.42	12.2	3.6 ± 1.0	11.3 ± 1.2	7.4 ± 1.6
	0.53	15.2	3.3 ± 0.7	12.1 ± 1.1	7.7 ± 1.3
	0.79	22.9	-0.7 ± 0.7	10.9 ± 1.1	5.1 ± 1.3

Table A.4. Results from the CAN-bus fuel-rate analysis for the curved track segments. The data represent vehicle speeds of 105 km/h (65 mph) and vehicle masses of 29,500 kg (65,000 lb).

Test Configuration	Separation Time [s]	Separation Distance [m]	Lead Truck Fuel Savings [%]	Trailing Truck Fuel Savings [%]	Platoon Fuel Savings [%]
Aligned	0.32	9.1	6.3 ± 0.7	9.1 ± 1.2	7.7 ± 1.3
	0.42	12.2	4.4 ± 0.6	9.4 ± 1.1	6.9 ± 1.3
	0.53	15.2	3.2 ± 0.7	9.2 ± 1.1	6.2 ± 1.3
	0.79	22.9	1.6 ± 0.7	7.7 ± 1.2	4.6 ± 1.4
	1.58	45.7	-1.3 ± 0.8	4.7 ± 1.2	2.4 ± 0.6
	2.71	78.6	1.4 ± 0.7	0.2 ± 1.2	0.1 ± 0.6
0.65 m Lateral Offset	0.32	9.1	3.7 ± 0.8	7.6 ± 1.3	5.7 ± 1.6
	0.42	12.2	2.4 ± 0.8	9.7 ± 1.2	6.1 ± 1.4
	0.53	15.2	1.1 ± 0.8	9.2 ± 1.2	5.1 ± 1.4
	0.79	22.9	0.6 ± 0.7	7.6 ± 1.2	4.1 ± 1.3
1.3 m Lateral Offset	0.32	9.1	5.7 ± 0.7	8.8 ± 1.2	7.2 ± 1.3
	0.42	12.2	3.6 ± 0.8	8.9 ± 1.2	6.2 ± 1.4
	0.53	15.2	4.0 ± 0.6	10.0 ± 1.1	7.0 ± 1.3
	0.79	22.9	-0.6 ± 0.6	7.5 ± 1.1	3.5 ± 1.3